The Physical Basis of Integrable Spin Models

Indrani Bose,
Department of Physics , Bose Institute ,
93/1, A.P.C. Road , Calcutta-700009, India

1st February 2008

Abstract

Integrable models are often constructed with real systems in mind. The exact solvability of the models leads to results which are unambiguous and provide the correct physical picture. In this review, we discuss the physical basis of some integrable spin models and their relevance in the study of real systems. The emphasis in the review is on physical understanding rather than on the mathematical aspects of integrability.

1 Introduction

The study of integrable models constitutes an important area of theoretical physics. Integrable models in condensed matter physics describe interacting many particle systems. The most prominent examples are interacting spin and electron systems which include several real materials of interest. Integrable models, because of their exact solvability, provide a complete and unambiguous understanding of the variety of phenomena exhibited by real systems. Integrability in the quantum case implies the existence of N conserved quantities where N is the number of degrees of freedom of the system. The corresponding operators including the Hamiltonian commute with each other. More specifically, integrable models are also described as exactly-solvable since the ground state energy and the excitation spectrum of the models can be determined exactly. Historically, the first example of the exact solvability of a many body problem was that of a spin$-\frac{1}{2}$ quantum spin chain [1]. The technique used to solve the eigenvalue problem is now known as the Bethe Ansatz (BA) named after Hans Bethe who formulated it. The demonstration of integrability, namely, the existence of N commuting operators can be made in the more general mathematical framework of the Quantum Inverse Scattering Method (QISM) [2]. The BA has been used extensively to obtain exact results for several quantum models in one dimension (1d). Examples include the Fermi and Bose gas models in which particles on a line interact through delta function potentials [3], the Hubbard model [4], 1d plasma which crystallises as a Wigner solid [5], the Lai-Sutherland model which includes the Hubbard model and a dilute magnetic model as special cases [6], the Kondo model [7], the single impurity Anderson model [8], the supersymmetric $t-J$ model ($J=2t$) etc [9]. The BA method has further been applied to derive exact results for classical lattice statistical models in 2d.

The BA denotes a particular form for the many-particle wave function. In a 1d system with pairwise interactions, a two particle scattering conserves the momenta individually due to the energy and momentum conservation constraints peculiar to 1d. Hence the scattering particles can either retain their original momenta or exchange them. In the case of two particles ($N=2$), the wave function has the form

$$\psi(x_1,x_2)=A_{12}e^{i(k_1x_1+k_2x_2)}+A_{21}e^{i(k_2x_1+k_1x_2)} \tag{1}$$

where x_1 , x_2 denote the locations of the two particles and k_1 , k_2 are the momentum variables. The wave function can alternatively be written as

$$\psi(x_1,x_2)=e^{i(k_1x_1+k_2x_2)}+e^{i\theta_{12}}e^{i(k_2x_1+k_1x_2)} \tag{2}$$

where θ_{12} is the scattering phase shift. The BA generalises the wave function (Eq.(1)) to the general case of N particles and is given by

$$\psi = \sum_P A(P) e^{i \sum_{j=1}^{N} k_{Pj} x_j}, x_1 < x_2 < .....x_N \tag{3}$$

The sum over P is a sum over all permutations of $1, ..., N$. The amplitude $A(P)$ is factorisable. Each $A(P)$ is a product of factors $e^{\theta_{ij}}$'s corresponding to each exchange of k_i 's required to go from the ordering $1, ..., N$ to the ordering P. An overall sign factor may arise depending on the parity of the permutation. The unknown variables θ_{ij} 's and k_i 's are obtained as solutions of coupled nonlinear equations. The factorisability condition is at the heart of the exact solvability of the eigenvalue problem. In the more general QISM approach, the so-called Yang-Baxter equation provides the condition for factorization of a multi-particle scattering matrix in terms of two-particle scattering matrices.

The traditional BA (Eq.(3)) is known as the Coordinate Bethe Ansatz (CBA). Over the years, the BA method has been generalised in different ways. The nested BA technique [3, 10] has been applied to study a system of particles with internal degrees of freedom. The state of a system of electrons is specified in terms of both the spatial positions as well as the spin indices of the electrons. The Asymptotic Bethe Ansatz [11] deals with a class of models in which the interaction between a pair of particles falls off as the inverse square of the distance between the particles. The Thermodynamic Bethe Ansatz method [12] is used to calculate thermodynamic quantities and is a finite temperature extension of the BA method. The Algebraic Bethe Ansatz (ABA) [13] has been developed in the powerful mathematical framework of the QISM. The ABA and CBA are equivalent in the sense that both lead to the same results for the energy eigenvalues. The CBA, however, does not provide knowledge of the correlation functions as the structure of the wave function is not sufficiently explicitly known. The QISM allows the calculation of the correlation functions in some cases [14]. The mathematical formalism is also much more systematic and general. One can further establish the existence of an infinite number ($N \to \infty$) of mutually commuting operators. The QISM moreover provides a prescription for the construction of integrable models. In this review, we will not discuss the mathematical aspects of integrable models for which a good number of reviews already exist [2, 15, 16, 17]. We focus on the physical basis of some integrable spin models in condensed matter physics and the useful physical insights derived from the solution of these models. The review is not meant to be exhaustive and should be supplemented by the references quoted at the end.

2 Spin models in 1d

The interest in 1d spin models arises from the fact that there are several real magnetic materials which can be described by such models. The spins interact via the Heisenberg exchange interaction and in many compounds the exchange interaction within a chain of spins is much stronger than that between chains. Thus the compounds effectively behave as linear chain systems. The most general exchange interaction Hamiltonian describing a chain of spins in which only nearest-neighbour (n.n.) spins interact is given by

$$H_{XYZ} = \sum_{i=1}^{N} \left[J_x S_i^x S_{i+1}^x + J_y S_i^y S_{i+1}^y + J_z S_i^z S_{i+1}^z \right] \tag{4}$$

where $S_i^\alpha (\alpha = x, y, z)$ is the spin operator at the lattice site i, N is the total number of sites and J_α denotes the strength of the exchange interaction. Consider the spins to be of magnitude $\frac{1}{2}$. The eigenvalue problems corresponding to the isotropic chain ($J_x = J_y = J_z = J$) and the longitudinally anisotropic chain ($J_x = J_y \neq J_z$) were originally solved using the CBA. Later, the same solutions were obtained using the formalism of QISM [13, 15]. Baxter [18]calculated the ground state energy of the fully anisotropic model (Eq.(4)) and Johnson, Krinsky and McCoy [19] found the excitation spectrum. The results were derived on the basis of a special relationship between the transfer matrix of the exactly-solved 2d classical lattice statistical eight vertex model and the fully anisotropic quantum spin Hamiltonian H_{XYZ} . Later, the same results were obtained by the ABA approach of the QISM. The Ising ($J_x = J_y = 0$) and the XY ($J_z = 0$) Hamiltonians are special cases of H_{XYZ} .

Consider the isotropic Heisenberg exchange interaction Hamiltonian in 1d

$$H = J\sum_{i=1}^{N} \overrightarrow{S}_i.\overrightarrow{S}_{i+1} \tag{5}$$

with periodic boundary conditions. The sign of the exchange interaction determines the favourable alignment of the n.n. spins. $J > 0$ corresponds to antiferromagnetic (AFM) exchange interaction due to which n.n. spins tend to be antiparallel. If $J < 0$ (equivalently, replace J by $-J$ in Eq.(5) with $J > 0$), the exchange interaction is ferromagnetic (FM) favouring a parallel alignment of n.n. spins. One can include a magnetic field term $-h\sum_{i=1}^{N} S_i^z$ in the Hamiltonian (Eq.(5)), where h is the strength of the field. Given a Hamiltonian , the quantities of interest are the ground state energy and the low-lying excitation spectrum. Knowledge of the latter enables one to calculate thermodynamic quantities like magnetization, specific heat and susceptibility at low temperatures. In the case of the FM Heisenberg Hamiltonian, the exact ground state has a simple structure. All the spins are parallel, i.e., they align in the same direction. The lowest excitation is a spin wave or magnon. The excitation is created by deviating a spin from its ground state arrangement and letting it propagate. For more than one spin deviation, one has continua of scattering states as well as bound complexes of magnons. In a bound complex, the spin deviations preferentially occupy n.n. lattice positions. The r-magnon bound state energy can be calculated using the BA [1]and the energy (in units of J) measured w.r.t. the ground state energy is

$$\epsilon = \frac{1}{r}(1 - cosK) \tag{6}$$

where K is the centre of mass momentum of the r magnons. The spin wave excitation energy is obtained for $r = 1$. The results can be generalised to the longitudinally anisotropic XXZ Hamiltonian. The multimagnon bound states were first detected in the quasi-1d magnetic system $CoCl_2.2H_2O$ [20]. Later improvements made it possible to observe even 14 magnon bound states [21].

In the case of the AFM isotropic Heisenberg Hamiltonian, the ground state is a singlet and the ground state wave function is a linear combination of all possible states in which half the spins are up and the other half down. The AFM ground state can be obtained from the FM ground state by creating $r = \frac{N}{2}$ magnons with momenta k_i and negative energies $-J(1 - cosk_i)$. Remember that the sign of the exchange integral is changed in going from ferromagnetism to antiferromagnetism. The highest energy state in the FM case ($r = \frac{N}{2}$) becomes the ground state in the AFM case. The BA equations can be recast in terms of the variables $z_i \equiv cot(\frac{k_i}{2})$ [22]:

$$Narctanz_i = \pi I_i + \sum_{j\neq i} arctan\left(\frac{z_i - z_j}{2}\right), i = 1, 2, ..., r \tag{7}$$

The Bethe quantum numbers I_i's are integers (half integers) for odd (even) r. For a state specified by $\{I_1, ..., I_r\}$, the solution $(z_1, ..., z_r)$ can be obtained from Eq. (7). The energy and the momentum wave number of the state are given by

$$\frac{E - E_F}{J} = -\sum_{i=1}^{r} \frac{2}{1 + z_i^2} \tag{8}$$

$$k = \pi r - \frac{2\pi}{N}\sum_{i=1}^{r} I_i \tag{9}$$

with $E_F = \frac{JN}{4}$. For the AFM ground state, the Bethe quantum numbers are given by

$$\{I_i\} = \left\{-\frac{N}{4} + \frac{1}{2}, -\frac{N}{4} + \frac{3}{2}, ..., \frac{N}{4} - \frac{1}{2}\right\} \tag{10}$$

In the thermodynamic limit $N \to \infty$, the exact ground state energy has been computed as

$$E_g = NJ(-ln2 + \frac{1}{4}) \tag{11}$$

The AFM ground state serves as the physical vacuum for the creation of elementary excitations. These excitations are not the spin-1 magnons but spin$-\frac{1}{2}$ spinons [23]. The spinons can be generated systematically by suitable modifications of the vacuum array of the BA quantum numbers (Eq.(2)) (for details see [22, 23]). For even N, spinons are always created in pairs, each such pair originating from the removal of one magnon from the ground state. Since the spinons are spin$-\frac{1}{2}$ objects, the lowest excitations consisting of a pair of spinons are four-fold degenerate , three triplet ($S = 1$) and one singlet ($S = 0$) excitations. The energy can be written as $E(k_1, k_2) = \epsilon(k_1) + \epsilon(k_2)$ where the spinon spectrum $\epsilon(k_i) = \frac{\pi}{2} \sin k_i$ and the total momentum $k = k_1 + k_2$. At a fixed total momentum k, one gets a continuum of scattering states. The lower boundary of the continuum is given by $\frac{\pi}{2} |sink|$ with one of the $k_i's = 0$. The upper boundary is obtained for $k_1 = k_2 = \frac{k}{2}$ and is given by $\pi \left|sin\frac{k}{2}\right|$. Figure 1 gives an example of a two-spinon configuration.

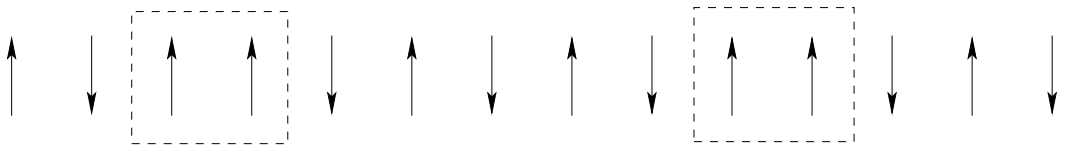

Figure 1. *A two-spinon configuration in an AFM chain.*

The BA results are obtained in the thermodynamic limit. In this limit, the energies and the momenta of the spinons just add up, showing that they do not interact. Since the spinons are excited in pairs, the total spin of the excited state is an integer. Inelastic neutron scattering study of the linear chain $S = \frac{1}{2}$ HAFM compound $KCuF_3$ has confirmed the existence of unbound spinon pair excitations [24]. It is to be noted that in the case of a ferromagnet, the low-lying excitation spectrum consists of a single magnon branch whereas the AFM spectrum is a two-spinon continuum with well-defined lower and upper boundaries.

The dynamical properties of a magnetic system are governed by the time-dependent pair correlation functions or their space-time double Fourier transforms known as dynamical correlation functions. An important time-dependent correlation function is

$$G(R,t) = \left\langle \overrightarrow{S}_R(t).\overrightarrow{S}_0(0) \right\rangle \tag{12}$$

The corresponding dynamical correlation function is the quantity measured in inelastic neutron scattering experiments. The differential scattering cross-section in such an experiment is given by

$$\frac{d^2\sigma}{d\Omega d\omega} \propto S^{\mu\mu}(\overrightarrow{q},\omega) = \frac{1}{N} \sum_R e^{i\overrightarrow{q}.\overrightarrow{R}} \int_{-\infty}^{+\infty} dt e^{i\omega t} \langle S_R^\mu(t) S_0^\mu(0) \rangle \tag{13}$$

where $\overrightarrow{q}$ and ω are the momentum wave vector and energy of the spin excitation and $\mu = x, y, z$. For a particular $\overrightarrow{q}$, the peak in $S^{\mu\mu}(\overrightarrow{q},\omega)$ occurs at a value of ω which gives the excitation energy. At $T = 0$,

$$S^{\mu\mu}(\overrightarrow{q},\omega) = \sum_\lambda M_\lambda^\mu \delta(\omega + E_g - E_\lambda) \tag{14}$$

$E_g(E_\lambda)$ is the energy of the ground (excited) state and

$$M_\lambda^\mu = 2\pi \left|\langle G| S^\mu(\overrightarrow{q}) |\lambda\rangle\right|^2 \tag{15}$$

is the transition rate between the singlet ($S_{tot} = 0$) ground state $|G\rangle$ and the triplet ($S_{tot} = 1$) states $|\lambda\rangle$ [25]. The exact calculation of the dynamical correlation functions in the BA formalism is not possible. Bougourzi et al [26] have used an alternative approach, based on the algebraic analysis of the completely integrable spin chain, and have calculated the exact 2-spinon part of the dynamical correlation function $S^{xx}(q,\omega)$ for the 1d $S = \frac{1}{2}$ AFM XXZ model. In this model, the Ising part of the XXZ Hamiltonian provides the dominant interaction. Karbach et al have [27]calculated the exact 2-spinon part of $S^{zz}(q,\omega)$ for the isotropic Heisenberg Hamiltonian. In both the cases, the size of the chain is infinite. The exact form of the 2-spinon

contribution to the dynamical correlation function $S^{xx}(q,\omega)$ of the $S=\frac{1}{2}$ XXZ HAFM chain is complicated and is given by

$$S^{xx}_{(2)}(q,\omega)=\frac{\omega_0}{8I\omega}\left[1+\sqrt{\frac{\omega^2-\chi^2\omega_0^2}{\omega^2-\omega_0^2}}\right]\sum_{c=\pm}\frac{\vartheta_A^2(\beta_-^c)}{\vartheta_d^2(\beta_-^c)}\frac{\left|tan(\frac{q}{2})\right|^{-c}}{W_c} \tag{16}$$

where $I=\frac{JK}{\pi}sinh\frac{\pi K'}{K}, \chi\equiv\frac{1-k'}{1+k'}$and $k,k'\equiv\sqrt{1-k^2}$ are the modulii of the elliptic integrals $K\equiv K(k), K'\equiv K(k')$. The anisotropy parameter $q=-exp(\frac{-\pi K'}{K})$ with $-\frac{J_z}{J_x}=\Delta=(\frac{q+q^{-1}}{2})$. Also,

$$W_\pm=\sqrt{\frac{\omega_0^4}{\omega^4}\chi^2-(\frac{T}{\omega^2}\pm cosq)^2} \tag{17}$$

$$T=\sqrt{\omega^2-\chi^2\omega_0^2}\sqrt{\omega^2-\omega_0^2} \tag{18}$$

$$\omega_0=\frac{2Isin(q)}{1+\chi} \tag{19}$$

$$\beta_-^c(q,\omega)=\frac{1+\chi}{2}F\left[arcsin(\frac{2I\omega W_c}{\chi(1+\chi)\omega_0^2}),\chi\right] \tag{20}$$

(F is the incomplete elliptic integral)

$$\vartheta_A^2(\beta)=exp(-\sum_{l=1}^{\infty}\frac{e^{\gamma l}}{l}\frac{cosh(2\gamma l)cos(t\gamma l)-1}{sinh(2\gamma l)cosh(\gamma l)}) \tag{21}$$

$\gamma=\frac{\pi K'}{K}, t\equiv\frac{2\beta}{K'}$ and $\vartheta_d(x)$ is a Neville theta function. The derivation of $S^{xx}_{(2)}(q,\omega)$ involves generating the 2-spinon states from the spinon vacuum, namely, the AFM ground state, with the help of spinon creation operators and expressing the spin fluctuation operator $S^\mu(q)$ in terms of the spinon creation operators. The 2-spinon part is expected to provide the dominant contribution to the dynamical correlation function (Eq. (14)). For example, in the case of the isotropic Heisenberg Hamiltonian, the 2-spinon excitations account for approximately 73% of the total intensity in $S^{zz}(q,\omega)$. The 2-spinon triplet excitations play a significant role in the low-temperature spin dynamics of quasi-1d AFM compounds like $KCuF_3, Cu(C_6D_5COO)_2.3D_2O, Cs_2CuCl_4$ and $Cu(C_4H_4N_2(NO_3)_2)$ [24, 28]. These excitations can be probed via inelastic neutron scattering and hence a knowledge of the exact dynamical correlation function is useful. The 2-spinon singlet excitations cannot be excited in neutron scattering because of selection rules (the spinon vacuum $|G\rangle$ is a singlet and the excited state $|\lambda\rangle$ in Eq.(15) is a triplet). Linear chain compounds like $CuGeO_3$ exhibit the spin-Peierls transition [29]. The transition gives rise to lattice distortion and consequently to a dimerization of the exchange interaction. Exchange interactions between successive pairs of spins alternate in strength. There is a tendency for the formation of dimers (singlets) across the strong bonds. One can construct an appropriate dynamical correlation function in which the dimer fluctuation operator (DFO) replaces the spin fluctuation operator $S^\mu(q)$. The DFO connects the AFM ground state to the 2-spinon singlet and not to the 2-spinon triplet.

Two well-known physical realizations of the 1d $S=\frac{1}{2}$ Ising-Heisenberg compounds are $CsCoCl_3$ and $CsCoBr_3$. Several inelastic neutron scattering measurements have been carried out on these compounds to probe the low-temperature spin dynamics [30]. In these compounds, the Ising part of the XXZ Hamiltonian is significantly dominant so that perturbation calculations around the Ising limit are feasible. Near the Ising limit, the exact 2-spinon dynamical correlation function $S^{xx}(q,\omega)$ is identical in the lowest order to the first-order perturbation result of Ishimura and Shiba (IS) [31]. The IS calculation provides physical insight on the nature of spinons. The Ising part of the XXZ Hamiltonian is the unperturbed Hamiltonian and the XY part constitutes the perturbation. The two-fold degenerate Néel states are the ground states of the Ising Hamiltonian. These two states serve as the "spinon vacuua". An excitation is created by flipping a block of adjacent spins from the spin arrangement in the Néel state. For example, in Figure 1, a block of seven spins is flipped in the Néel state. The block of overturned spins gives rise to two parallel spin pairs at its boundary with the unperturbed Néel configuration. It is these domain walls or kink solitons which

are the equivalents of spinons. A 2-spinon excited state ($S^z_{tot} = 1$) is obtained as a linear superposition of states in which an odd number ν ($\nu = 1, 3, 5, ...$) of spins is overturned in the Néel configuration. In each such state, both the domain walls have equal spin orientations with the spins pointing up. The excitation continuum of two spinons is obtained in first order perturbation theory. The lineshapes of $S^{xx}(q, \omega)$ observed in experiments are highly asymmetric with a greater concentration of intensity near the spectral threshold and a tail extending to the upper boundary of the continuum. The exact 2-spinon part of $S^{xx}(q, \omega)$ has also an asymmetric shape in agreement with experimental data. The first order perturbation-theoretic result of IS for $S^{xx}(q, \omega)$ fails to reproduce the asymmetry. A second-order perturbation calculation leads to greater asymmetry in the lineshapes [32]. Furthermore, in the framework of a first order perturbation theory, the effects of full anisotropy ($J_x \neq J_y \neq J_z$), next-nearest-neighbour coupling, interchain coupling and exchange mixing have been shown to give rise to asymmetry in lineshapes [33].

Recently, a large number of studies have been carried out on a class of models in which the interaction between spins falls off as the inverse-square of the distance between them. A lattice model which belongs to this class is known as the Haldane-Shastry model [34] the Hamiltonian of which is given by

$$H = J \sum_{i<j} \frac{P_{ij}}{d(i-j)^2} \tag{22}$$

where $d(l) = (\frac{N}{\pi}) \left| sin \frac{\pi l}{N} \right|$is the chord distance between the pair of spins separated by l sites on a ring with N equally spaced spins. P_{ij} is the spin exchange operator, $P_{ij} = (2 \overrightarrow{S}_i . \overrightarrow{S}_j + \frac{1}{2})$. The model is exactly solvable and the key results are: the ground state has a form similar to the fractional quantum Hall ground state, the ground state is a QSL and the elementary excitations are the spin$-\frac{1}{2}$ spinons obeying fractional statistics, the thermodynamics as well as the various dynamical correlation functions can be calculated exactly. The latter calculations are possible because of the simple structure of the eigenspectrum.

A correct analysis of the BA equations for the $S = \frac{1}{2}$ HAFM in 1d gave rise to the concept of spinons which has subsequently been verified in experiments. Approximate methods like spin wave theory fail to predict the spinon continuum thus pointing to the importance of integrable models in providing the correct physical picture. The existence of spinons in dimension greater than one is a highly debatable issue. No precise statement can be made due to the lack of exact results in $d > 1$. The issue is of considerable significance in connection with the resonating-valence-bond (RVB) theory of high temperature superconductivity. In a valence bond (VB) state, pairs of spins are in singlet spin configurations (a singlet is often termed as a VB). The RVB state is a coherent linear superposition of VB states. In 1973, Anderson [35] in a classic paper suggested that the ground state of the $S = \frac{1}{2}$ HAFM on the frustrated triangular lattice is a RVB state. The RVB state is a singlet (total spin is zero) and is often described as a quantum spin liquid (QSL) since translational as well as rotational symmetries are preserved in the state. The RVB state is spin disordered and the two-spin correlation function has an exponential decay as a function of the distance between the spins. Interest in the RVB state revived after the discovery of high temperature superconductivity in 1987[36]. The common structural ingredient of the high$-T_C$ cuprate systems is the copper-oxide (CuO_2) plane which ideally behaves as a $S = \frac{1}{2}$ HAFM defined on a square lattice. It is largely agreed that the ground state ($T = 0$) has AFM long range order (LRO). The low-lying excitations are the conventional $S = 1$ magnons. In the spinon picture, a magnon is a pair of confined spinons. The spinons cannot move apart from each other unlike in 1d. The cuprates exhibit a rich phase diagram as a function of the dopant concentration. On doping, positively charged holes are introduced in the CuO_2 plane. The holes are mobile in a background of antiferromagnetically interacting spins. The motion of holes acts against antiferromagnetism and the AFM LRO is rapidly destroyed as the concentration of holes increases. The resulting spin disordered state has been speculated to be a RVB state. In close analogy with the $S = \frac{1}{2}$ HAFM chain, the low-lying spin excitations in the RVB state are pairs of spinons. The spinons are created by breaking a VB. The spinons are not confined as in the case of an ordered ground state but separate via a rearrangement of the VBs. The spinons have spin $\frac{1}{2}$ and charge 0. The charge excitations in a RVB state are known as holons with charge $+e$ and spin 0. Holons are created on doping the RVB state, i.e., replacing electrons by holes. Spinons and holons are best decribed as topological excitations in a QSL. The key feature of the doped RVB state is that of spin-charge separation, i.e., the spin and charge excitations are decoupled entities. Spin-charge separation can be rigorously demonstrated in the case of interacting electron systems in 1d known by the general name

of Luttinger Liquids (LLs). The Hubbard model in 1d is the most well-known example of a LL. The model is integrable and the BA results for the excitation spectrum confirm that the spinons and the holons are the elementary excitations [36, 37].

Coming back to the RVB state, there has been an intensive search for spin models in 2d with RVB states as exact ground states. Recent calculations show that there is AFM LRO in the ground state of the $S = \frac{1}{2}$ HAFM on the triangular lattice, contrary to Anderson's original conjecture [38]. Frustrated spin models with n.n. as well as non-n.n. exchange interactions have been constructed for which the RVB states are the exact ground states in certain parameter regimes [39]. These are short-ranged RVB states with the VBs forming between n.n. spin pairs. The spinon excitation spectrum in this case is gapped. A model which captures the low energy dynamics in the RVB scenario is the Quantum Dimer Model (QDM)[40]. The Hamiltonian of the model defined on a square lattice is given by

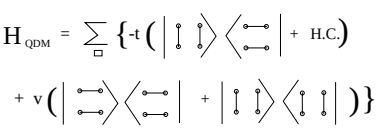

(23)

where the solid lines represent dimers (VBs) and the sum runs over all the plaquettes of the lattice. The first term of the Hamiltonian is the kinetic part representing the flipping of a pair of parallel dimers on the two bonds of a plaquette to the other possible orientation, i.e., from horizontal to vertical and vice versa. The second term counts the number of flippable pairs of dimers in any dimer configuration and is analogous to the potential term of the Hamiltonian. The ground state of the QDM on the square lattice is not, however, a QSL except at the special point $t = V$. Moessner and Sondhi [41] have studied the QDM on the triangular lattice and shown that, in contrast to the square lattice case , the ground state is a RVB state with deconfined, gapped spinons in a finite range of parameters. Recently, some microscopic models of 2d magnets have been proposed [42] the low-lying excitations of which are of three types: spinons, holons and "vortex-like" excitations with no spin and charge, dubbed as visons. Some of these models are related to the QDM. Two integrable models [42, 43] have been constructed which share common topological features with the microscopic models in 2d and have applications in fault-tolerant quantum computation. The models ,however, cannot resolve the issue of spinons in 2d as quantum numbers like the total S^z are not conserved in these models. The search for microscopic models in 2d, with spinons as elementary excitations, acquires particular significance in the light of recent experimental evidence of the spinon continuum in the 2d frustrated quantum antiferromagnet Cs_2CuCl_4 [44]. The ground state of this compound is expected to be a QSL with spinons and not magnons as elementary excitations. Exactly solvable models in 2d are needed for a clear understanding of the origin of the experimentally observed spinon continuum.

Real materials are often anisotropic in character. The anisotropy may be present in the exchange interaction Hamiltonian itself or there may be additional terms in the Hamiltonian corresponding to different types of anisotropy. A well-known anisotropic interaction, present in many AFM materials, is the Dzyaloshinskii-Moriya (DM) interaction with the general form

$$H_{DM} = \overrightarrow{D}.(\overrightarrow{S}_i \times \overrightarrow{S}_j) \tag{24}$$

Moriya [45] provided the microscopic basis of the DM interaction by extending Anderson's superexchange theory to include the spin-orbit interaction. The DM coupling acts to cant the spins because the coupling energy is minimised when the two spins are perpendicular to each other. Some examples of materials with DM interaction include the quasi-2d compound Cs_2CuCl_4 [44], the CuO_2 planes of the undoped cuprate system La_2CuO_4 [46], the quasi-1d compound Cu-Benzoate [47] etc. The DM canting of spins is responsible for the small ferromagnetic moment of the CuO_2 planes even though the dominant in-plane exchange interaction is AFM in nature. Alcaraz and Wreszinski [48] have shown that the XXZ quantum Heisenberg chain (both FM and AFM) with DM interaction is equivalent to the XXZ Hamiltonian with modified boundary conditions and anisotropy parameter $\frac{J_z}{J_x}$. The DM interaction is assumed to be of the form

$$H_{DM}(\Delta) = -\frac{\Delta}{2}\sum_{i=1}^{N}(\sigma_i^x\sigma_{i+1}^y - \sigma_i^y\sigma_{i+1}^x) \tag{25}$$

,i.e., the vector $\overrightarrow{D}$ in Eq.(23) is in the z-direction. The new anisotropy parameter is $\frac{\delta}{\sqrt{1+\Delta^2}}$ where δ is the anisotropy parameter of the original XXZ Hamiltonian. With changed boundary conditions, the model is still BA solvable. In fact, in the thermodynamic limit ($N \to \infty$), the boundary conditions do not affect the critical behaviour. Thus, the Hamiltonian, which includes both the XXZ Hamiltonian and the DM interaction, has the same critical properties and the phase diagram as the XXZ Hamiltonian with the anisotropy parameter $\frac{\delta}{\sqrt{1+\Delta^2}}$.

We next turn our attention to spin$-S$ ($S > \frac{1}{2}$) quantum spin chains. The spin$-S$ Heisenberg exchange interaction Hamiltonian in 1d is not integrable. A family of Heisenberg-like models has been constructed for $S = 1, \frac{3}{2}, 2, \frac{5}{2}, ...$ etc. for which the spin$-S$ quantum Hamiltonian is given by

$$H_s = \sum_i Q(\overrightarrow{S}_i.\overrightarrow{S}_{i+1}) \tag{26}$$

where $Q(x)$ is a polynomial of degree $2S$ [49]. With this generalization, the spin$-S$ quantum spin chains are integrable. The integrable models, however, do not distinguish between half-odd integer and integer spins. In both the cases, the integrable models have gapless excitation spectrum. For half-odd integer AFM Heisenberg spin chains (with only the bilinear exchange interaction term), the Lieb-Schultz-Mattis (LSM) theorem [50] states that the excitation spectrum is gapless. The theorem cannot be proved for AFM integer spin chains. Haldane in 1983 pointed out the difference between the half-odd integer and integer AFM Heisenberg spin chains and made the conjecture that integer spin chains have a gap in the excitation spectrum [51]. Integer spin quantum antiferromagnets in 1d have been widely studied analytically, numerically and experimentally and Haldane's conjecture has turned out to be true. There are several examples of quasi-1d $S = 1$ AFM materials which exhibit the Haldane gap. Some of the most widely studied materials are $CsNiCl_3, Ni(C_2H_8N_2)_2NO_2(ClO_4)$ (NENP), Y_2BaNiO_5 etc. Recently, experimental evidence of a $S = 2$ antiferromagnet which exhibits the Haldane gap has been obtained. In this compound the manganese ions form effective $S = 2$ spins and are coupled in a quasi-1d chain [52]. Integrable models of integer spin chains do not reproduce the Haldane gap but are of considerable interest since they provide exact information about the phase diagram of generalised integer spin models. Consider the generalised Hamiltonian for an AFM $S = 1$ chain:

$$H = \sum_i \left[cos\theta(\overrightarrow{S}_i.\overrightarrow{S}_{i+1}) + sin\theta(\overrightarrow{S}_i.\overrightarrow{S}_{i+1})^2\right] \tag{27}$$

with θ varying between 0 and 2π. The biquadratic term has been found to be relevant in some real integer-spin materials. There are two gapped phases: the Haldane phase for $-\frac{\pi}{4} < \theta < \frac{\pi}{4}$and a dimerised phase for $-\frac{3\pi}{4} < \theta < -\frac{\pi}{4}$ [53]. At $\theta = -\frac{\pi}{4}$, the model is integrable and the gap vanishes to zero. This point separates the two gapped phases, Haldane and dimerised, which have different symmetry properties. Thus a quantum phase transition occurs at $\vartheta = -\frac{\pi}{4}$ from the Haldane to the dimerised phase. The integrable model provides exact location of the transition point. The point $\theta = \frac{\pi}{4}$corresponds to the Hamiltonian which is a sum over permutation operators and is again exactly solvable. The Haldane phase includes the isotropic Heisenberg chain ($\theta = 0$) and the Affleck-Kennedy-Lieb-Tasaki (AKLT) Hamiltonian ($tan\theta_{VBS} = \frac{1}{3}$) [54]. The latter model is not integrable but the ground state is known exactly. The ground state is described as a valence bond solid (VBS) state in which a VB (singlet) covers every link of the chain. Since the gap does not become zero for $0 \leq \theta \leq \theta_{VBS}$, there is no phase transition in going from one limiting Hamiltonian to the other. Thus the isotropic Heisenberg and AKLT chains are in the same phase.

The doped cuprate systems exhibit a variety of novel phenomena in their insulating, metallic and superconducting phases. A full understanding of these phenomena is as yet lacking. There is currently a strong research interest in doped spin systems. The idea is to look for simpler spin systems in which the consequences of doping can be studied in a less ambiguous manner. The spin-1 HG nickelate compound Y_2BaNiO_5 can be doped with holes on replacing the off-chain Y^{3+} ions by Ca^{2+} ions. Inelastic neutron

scattering (INS) measurements on the doped compound provide evidence for the appearance of new states in the HG [55]. The structure factor $S(q)$, obtained by integrating the dynamical correlation function $S(q,\omega)$ over ω, acquires an incommensurate, double-peaked form in the doped state [56]. Frahm et al [57] have constructed an integrable model describing a doped spin-1 chain. In the undoped limit, the spectrum is gapless and so the HG of the integer spin system is not reproduced. It is, however, possible to reintroduce a gap in the continuum limit where a field-theoretical description of the model is possible. The model has limited relevance in explaining the physical features of the doped nickelate compound. Another interesting study relates to the appearance of magnetization plateaus in the doped $S = 1$ integrable model [58]. The location of the plateaus depends on the concentration of holes. Experimental evidence of this novel phenomenon has not been obtained so far.

An electron in a solid, localised around an atomic site, has three degrees of freedom charge, spin and orbital. The orbital degree of freedom is relevant to several transition metal oxides which include the cuprate and manganite systems. The latter compounds on doping exhibit the phenomenon of colossal magnetoresistance in which there is a huge change in electrical resistivity on the application of a magnetic field. The manganites like the cuprates have a rich phase diagram as a function of the dopant concentration [59]. We now give a specific example of the orbital degree of freedom. The Mn^{3+} ion in the manganite compound $LaMnO_3$ has four electrons in the outermost $3d$ energy level. The electrostatic field of the neighbouring oxygen ions splits the 3d energy level into two sublevels, t_{2g} and e_g. Three of the four electrons occupy the three t_{2g} orbitals d_{xy}, d_{yz}, d_{zx} and the fourth electron goes to the e_g-sublevel containing the two orbitals $d_{x^2-y^2}$ and $d_{3z^2-r^2}$. The fourth electron thus has an orbital degree of freedom as it has two possible choices for occupying an orbital. The four electrons have the same spin orientation to minimise the electrostatic repulsion energy according to the Hund's rule. The total spin is thus $S = 2$. The orbital degree of freedom is described by the pseudospin $\overrightarrow{T}$ such that $T_z = \frac{1}{2}(-\frac{1}{2})$ when the $d_{x^2-y^2}$ ($d_{3z^2-r^2}$) orbital is occupied. The three components of the pseudospin satisfy commutation relations similar to those of the spin components. The e_g doublet is further split into two hyperfine energy levels due to the well-known Jahn-Teller (JT) effect. In concentrated systems, the JT effect can lead to orbital ordering below an ordering temperature. In the antiferromagnetically ordered Néel state, the spins are alternately up and down. Similarly, in the case of antiferroorbital ordering, the occupied orbitals alternate in type at successive sites of the lattice. The orbital degree of freedom is frozen as a result. Apart from the JT mechanism of orbital ordering, there is an exchange mechanism which may lead to orbital order. The exchange mechanism is a generalisation of the usual superexchange to the case of orbital degeneracy. Starting from the degenerate Hubbard model, in which there are two degenerate orbitals at each site, one can derive the following generalised exchange Hamiltonian [60]:

$$H = \sum_{ij} \left\{ J_1 \overrightarrow{S}_i . \overrightarrow{S}_j + J_2 \overrightarrow{T}_i . \overrightarrow{T}_j + J_3 (\overrightarrow{S}_i . \overrightarrow{S}_j)(\overrightarrow{T}_i . \overrightarrow{T}_j) \right\} \tag{28}$$

Consider the case $J_1 = J_2 = J$. For $J_3 = 0$, two independent Heisenberg-like Hamiltonians are obtained which are BA solvable. At the Kolezhuk-Mikeska point, $\frac{J_3}{J} = \frac{4}{3}$, the ground state is exactly known [61]. The point $\frac{J_3}{J} = 4$ is integrable and there are three gapless excitation modes. The compounds $Na_2Ti_2Sb_2O$ and NaV_2O_5 are examples of materials in 1d with coupled spin and orbital degrees of freedom [62]. These systems have been described by anisotropic versions of the Hamiltonian in Eq.(28) but without adequate agreement with experiments. The elementary excitations in the orbital sector are the orbital waves or "orbitons". An excitation of this type is created in the orbitally ordered state by changing the occupied orbital at a site and letting the defect propagate in the solid. The excitations are analogous to the spin waves or magnons in a magnetically ordered solid. Experimental evidence of orbital waves has recently been obtained in the manganite compound $LaMnO_3$ through Raman scattering measurements [63, 64]. As discussed before, integrable spin models provide important links between theory and experiments. A similar scenario in the case of systems with coupled spin and orbital degrees of freedom is yet to develop.

3 Ladder models

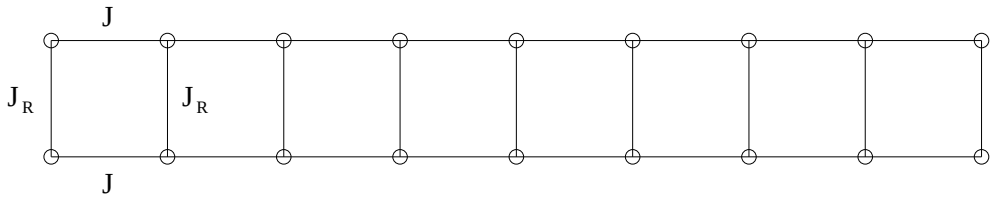

Figure 2. *A two-chain ladder. The rung and intra-chain n.n. exchange interactions are of strength J_R and J respectively.*

The simplest ladder model consists of two chains coupled by rungs (Figure 2). In general, the ladder may consist of n chains coupled by rungs. In the spin ladder model, each site of the ladder is occupied by a spin (in general of magnitude $\frac{1}{2}$) and the spins interact via the Heisenberg AFM exchange interaction. In the doped spin ladder model, some of the sites are empty, i.e., occupied by holes. The holes can move in the background of interacting spins. There are two major reasons for the considerable research interest in ladders. Powerful techniques like the BA and bosonization are available for the study of 1d many body systems whereas practically very few rigorous results are known for 2d systems. Ladders provide a bridge between 1d and 2d physics and are ideally suited to study how the electronic and magnetic properties change as one goes from a single chain to the square lattice. The unconventional properties of the CuO_2 planes of the cuprate systems are the main reason for the significant interest in 2d many body systems. Many of these properties are ascribed to strong correlation effects. Ladders are simpler systems in which some of the issues associated with strong correlation can be addressed in a more rigorous manner. The second motivation for the study of ladder systems is that several such systems have been discovered in the recent past. In the following, we describe in brief some of the major physical properties of ladders. There are two exhaustive reviews on ladders which provide more detailed information [65, 66].

Consider a two-chain spin ladder described by the AFM Heisenberg exchange interaction Hamiltonian

$$H = \sum_{\langle ij \rangle} J_{ij} \overrightarrow{S}_i . \overrightarrow{S}_j \tag{29}$$

The n.n. intra-chain and the rung exchange interactions are of strength J and J_R respectively. When $J_R = 0$, one obtains two decoupled AFM spin chains for which the excitation spectrum is known to be gapless. For all $\frac{J_R}{J} > 0$, a gap (the so-called spin gap (SG)) opens up in the spin excitation spectrum. The result is easy to understand in the simple limit in which the exchange coupling J_R along the rungs is much stronger than the coupling J along the chains. The intra-chain coupling may thus be treated as perturbation. When $J = 0$, the exact ground state consists of singlets along the rungs. The ground state energy is $-\frac{3J_R N}{4}$, where N is the number of rungs in the ladder. The ground state has total spin $S = 0$. In first order perturbation theory, the correction to the ground state energy is zero. A $S = 1$ excitation may be created by promoting one of the rung singlets to a $S = 1$ triplet. The weak coupling along the chains gives rise to a propagating $S = 1$ magnon. In first order perturbation theory, the dispersion relation is

$$\omega(k) = J_R + Jcosk \tag{30}$$

where k is the momentum wave vector. The SG defined as the minimum excitation energy is given by

$$\Delta_{SG} = \omega(\pi) \simeq (J_R - J) \tag{31}$$

The two-spin correlations decay exponentially along the chains showing that the ground state is a quantum spin liquid (QSL). The magnons can further form bound states. Experimental evidence of two-magnon bound states has been obtained in the $S = \frac{1}{2}$two-chain ladder compound $Ca_{14-x}La_xCu_{24}O_{41}$ ($x = 5$ and 4) [67]. The family of compounds $Sr_{n-1}Cu_{n+1}O_{2n}$ consists of planes of weakly-coupled ladders of $\frac{n+1}{2}$chains [68]. For $n = 3$ and 5, respectively, one gets the two-chain and three-chain ladder compounds $SrCu_2O_3$ and $Sr_2Cu_3O_5$ respectively. For the first compound, experimental evidence of the SG has been obtained. The

latter compound has properties similar to those of the 1d Heisenberg AFM chain [69]. A recent example of a spin ladder belonging to the organic family of materials is the compound $(C_5H_{12}N)_2CuBr_4$, a ladder system with strong rung coupling ($\frac{J_R}{J} \simeq 3.5$) [70]. The phase diagram of the AFM spin ladder in the presence of an external magnetic field is particularly interesting. In the absence of the magnetic field and at $T = 0$, the ground state is a QSL with a gap in the excitation spectrum. At a field H_{c_1}, there is a transition to a gapless Luttinger Liquid (LL) phase ($g\mu_B H_{c_1} = \Delta_{SG}$, the spin gap, μ_B is the Bohr magneton and g the Landé splitting factor). There is another transition at an upper critical field H_{c_2} to a fully polarised FM state. Both H_{c_1} and H_{c_2} are quantum critical points. The quantum phase transition from one ground state to another is brought about by changing the magnetic field. At small temperatures, the behaviour of the system is determined by the crossover between two types of critical behaviour: quantum critical behaviour at $T = 0$ and classical critical behaviour at $T \neq 0$. Quantum effects are persistent in the crossover region at small finite temperatures and such effects can be probed experimentally. In the case of the ladder system $(C_5H_{12}N)_2CuBr_4$, the magnetization data obtained experimentally exhibit universal scaling behaviour in the vicinity of the critical fields H_{c_1} and H_{c_2}. In the gapless regime $H_{c_1} < H < H_{c_2}$, the ladder model can be mapped onto an XXZ chain the thermodynamic properties of which can be calculated exactly by the BA. The theoretically computed magnetization M versus magnetic field h curve is in excellent agreement with the experimental data. Organic spin ladders provide ideal testing grounds for the theories of quantum phase transitions. For inorganic spin ladder systems, the value of H_{c_1} is too high to be experimentally accessible.

Bose and Gayen [71] have studied a frustrated two-chain spin model with diagonal couplings. The intrachain and diagonal spin-spin interactions are of equal strength J. It is easy to show that for $J_R \geq 2J$, the exact ground state consists of singlets (dimers) along the rungs with the energy $E_g = -\frac{3J_R N}{4}$ where N is the number of rungs. Xian [72] later pointed out that as long as $\frac{J_R}{J} > \left(\frac{J_R}{J}\right)_c \simeq 1.401$, the rung dimer state is the exact ground state. At $\frac{J_R}{J} = \left(\frac{J_R}{J}\right)_c$, there is a first order transition from the rung dimer state to the Haldane phase of the $S = 1$ chain. Kolezhuk and Mikeska [73] have constructed a class of generalised $S = \frac{1}{2}$ two-chain ladder models for which the ground state can be determined exactly. The Hamiltonian H is a sum over plaquette Hamiltonians and each such Hamiltonian contains various two-spin as well as four-spin interaction terms. They have further introduced a toy model which has a rich phase diagram in which the phase boundaries can be determined exactly.

The standard spin ladder models with bilinear exchange are not integrable. For integrability, multispin interaction terms have to be included in the Hamiltonian. Some integrable ladder models have already been constructed [74]. We discuss one particular model proposed by Wang [75]. The Hamiltonian is given by

$$\begin{aligned} H &= \frac{J_1}{4}\sum_{i=1}^{N}[\overrightarrow{\sigma}_j.\overrightarrow{\sigma}_{j+1} + \overrightarrow{\tau}_j.\overrightarrow{\tau}_{j+1}] + \frac{J_2}{2}\sum_{j=1}^{N}\overrightarrow{\sigma}_j.\overrightarrow{\tau}_j \\ &+ \frac{U_1}{4}\sum_{j=1}^{N}(\overrightarrow{\sigma}_j.\overrightarrow{\sigma}_{j+1})(\overrightarrow{\tau}_j.\overrightarrow{\tau}_{j+1}) + \frac{U_2}{4}\sum_{j=1}^{N}(\overrightarrow{\sigma}_j.\overrightarrow{\tau}_j)(\overrightarrow{\sigma}_{j+1}.\overrightarrow{\tau}_{j+1}) \end{aligned} \tag{32}$$

where $\overrightarrow{\sigma}_j$ and $\overrightarrow{\tau}_j$ are the Pauli matrices associated with the site j of the upper and lower chains respectively. N is the total number of rungs in the system. The ordinary spin ladder Hamiltonian is obtained from Eq. (32) when the four spin terms are absent, i.e., $U_1 = U_2 = 0$. For general parameters J_1, J_2, U_1 and U_2, the model is non-integrable. The integrable cases correspond to $U_1 = J_1, U_2 = 0$ or $U_1 = J_1, U_2 = -\frac{J_1}{2}$. Without loss of generality one can put $J_1 = U_1 = 1, J_2 = J$ and $U_2 = U$. For $U = 0$, the Hamiltonian (32) reduces to

$$H = \frac{1}{4}\sum_{j=1}^{N}(1 + \overrightarrow{\sigma}_j.\overrightarrow{\sigma}_{j+1})(1 + \overrightarrow{\tau}_j.\overrightarrow{\tau}_{j+1}) + \frac{J}{2}\sum_{j=1}^{N}(\overrightarrow{\sigma}_j.\overrightarrow{\tau}_j - 1) + \frac{1}{2}(J - \frac{1}{2})N \tag{33}$$

Three quantum phases are possible. For $J > J_+^c = 2$, the system exists in the rung dimerised phase. The ground state is a product of singlet rungs. The SG is given by $\Delta_{SG} = 2(J - 2)$. For $J_+^c > J > J_-^c$, a gapless phase is obtained with three branches of gapless excitations. J_+^c is the quantum critical point at which a QPT from the dimerised phase to the gapless phase occurs. In the vicinity of the quantum critical point, the susceptibility and the specific heat can be calculated using the thermodynamic BA. From the low-temperature expansion of the thermodynamic BA equation, one obtains

$$C \sim T^{\frac{1}{2}}, \chi \sim T^{-\frac{1}{2}} \tag{34}$$

which are typical of quantum critical behaviour. In the presence of an external magnetic field h, the magnetic field can be tuned to drive a QPT at the quantum critical point $h_c = 2(J-2)$ from the gapless phase to a gapped phase. The third quantum phase ($h = 0$) is obtained for $J < J_-^c = -\frac{\pi}{4\sqrt{3}} + \frac{ln3}{4}$. This is a gapless phase with two branches of gapless excitations. For $U = -\frac{1}{2}$, a similar phase diagram is obtained. Note that the ladder model may equivalently be considered as a spin-orbital model with $\overrightarrow{\sigma}$ and $\overrightarrow{\tau}$ representing the spin and the pseudospin.

Doped ladder models are toy models of strongly correlated systems [65]. In these systems, the double occupancy of a site by two electrons, one with spin up and the other with spin down, is prohibited due to strong coulomb correlations. In a doped spin system, there is a competition between two processes: hole delocalization and exchange energy minimization. A hole moving in an antiferromagnetically ordered spin background, say, the Néel state, gives rise to parallel spin pairs which raise the exchange interaction energy of the system. The questions of interest are: whether a coherent motion of the holes is possible, whether two holes can form a bound state, the development of superconducting (SC) correlations, the possibility of phase separation of holes etc. Some of these issues are of significant relevance in the context of doped cuprate systems in which charge transport occurs through the motion of holes [76]. In the SC phase, the holes form bound pairs with possibly d-wave symmetry. Several proposals have been made so far on the origin of hole binding but there is as yet no general consensus on the actual binding mechanism. The doped cuprate systems exist in a 'pseudogap' phase before the SC phase is entered. In fact, some cuprate systems also exhibit SG. As already mentioned, the doped two-chain ladder systems are characterised by a SG. The issue of how the gap evolves on doping is of significant interest. The possibility of binding of hole pairs in a two-chain ladder system was first pointed out by Dagotto et al [77]. In this case, the binding mechanism is not controversial and can be understood in a simple physical picture. Again, consider the case $J_R \gg J$, i.e., a ladder with dominant exchange interactions along the rungs. In the ground state, the rungs are mostly in singlet spin configurations. On the introduction of a single hole, a singlet spin pair is broken and the corresponding exchange interaction energy is lost. When two holes are present, they prefer to be on the same rung to minimise the loss in the exchange interaction energy. The holes thus form a bound pair. In the more general case, detailed energy considerations show that the two holes tend to be close to each other and effectively form a bound pair. For more than two holes, several calculations suggest that considerable SC pairing correlations develop in the system on doping. True superconductivity can be obtained only in the bulk limit. Theoretical predictions motivated the search for ladder compounds which can be doped with holes. Much excitement was created in 1996 when the ladder compound $Sr_{14-x}Ca_xCu_{24}O_{41}$ was found to become SC under pressure at $x = 13.6$ [78]. The transition temperature T_c is $\sim 12K$ at a pressure of $3GPa$. As in the case of cuprate systems, bound pairs of holes are responsible for charge transport in the SC phase. Experimental results on doped ladder compounds point out strong analogies between the doped ladder and cuprate systems [65].

The strongly correlated doped ladder system is described by the t-J Hamiltonian

$$H_{t-J} = -\sum_{\langle ij\rangle,\sigma} t_{ij}(\widetilde{C}_{i\sigma}^{+}\widetilde{C}_{j\sigma} + H.C.) + \sum_{\langle ij\rangle} J_{ij}(\overrightarrow{S}_i.\overrightarrow{S}_j - \frac{1}{4}n_i n_j) \tag{35}$$

The $\widetilde{C}_{i\sigma}^{+}$ and $\widetilde{C}_{i\sigma}$ are the electron creation and annihilation operators which act in the reduced Hilbert space (no double occupancy of sites),

$$\begin{aligned} \widetilde{C}_{i\sigma}^{+} &= C_{i\sigma}^{+}(1-n_{i-\sigma}) \\ \widetilde{C}_{i\sigma} &= C_{i\sigma}(1-n_{i-\sigma}) \end{aligned} \tag{36}$$

where σ is the spin index and n_i, n_j are the occupation numbers of the ith and jth sites respectively. The first term in Eq.(35) describes the motion of holes with hopping integrals t_R and t for motion along the rung and chain respectively. In the standard $t-J$ ladder model, i and j are n.n. sites. The second term contains the usual AFM Heisenberg exchange interaction Hamiltonian. The $t-J$ model thus describes the

motion of holes in a background of antiferromagnetically interacting spins. A large number of studies have been carried out on $t-J$ ladder models. These are reviewed in Refs. [65, 66]. We describe briefly some of the major results. The SG of the undoped ladder changes discontinuously on doping. Remember that the SG is the difference in energies of the lowest triplet excitation and the ground state. In the doped state, there are two distinct triplet excitations. One triplet excitation is that of the undoped ladder obtained by exciting a rung singlet to a rung triplet. A new type of triplet excitation is possible when at least two holes are present. On the introduction of two holes in two rung singlets, a pair of free spin$-\frac{1}{2}$'s is obtained which combines to give rise to a singlet ($S=0$) or a triplet ($S=1$) state. The triplet configuration of the two free spins corresponds to the second type of triplet excitation. The SG of this new excitation is unrelated to the SG of the magnon excitation. The true SG is the one which has the lowest value in a particular parameter regime.

The low energy modes of a ladder system are characterised by their spin. Singlet and triplet excitations correspond to charge and spin modes respectively. In each sector, the hole may further be in a bonding or antibonding state with opposite parities. We consider only the even parity sector to which the lowest energy excitations belong. In both the $S=0$ and $S=1$ sectors, an excitation continuum with well-defined boundaries is present. The $S=0$ and the $S=1$ continua are degnerate in energy. A bound state branch with $S=0$ splits off below the continuum the lowest energy of which corresponds to the c.o.m. momentum wave vector $K=0$ [79, 80]. Thus the two-hole ground state is in the singlet sector and corresponds to a bound state of two holes with $K=0$. The bound state has $d-$wave type symmetry. Within the bound state branch, excitations with energy infinitesimally close to the ground state are possible. These excitations are the charge excitations since the total spin is still zero and the charge excitation spectrum is gapless. The lowest spin excitations in a wide parameter regime are between the $S=0$ ground state and the lowest energy state in the $S=1$ continuum [81]. The continuum does not exist in the undoped ladder and so the SG evolves discontinuously on doping in this parameter regime. A suggestion has, however, been made that the lowest triplet excitation is a bound state of a magnon with a pair of holes [82]. In summary, the two-chain ladder model has the feature that the charge excitation is gapless but the spin excitation has a gap. This is the Luther-Emery phase and is different from the LL phase in which both the spin and charge excitations are gapless.

Bose and Gayen have derived several exact, analytical results for the ground state energy and the low-lying excitation spectrum of the frustrated $t-J$ ladder doped with one and two holes. The undoped ladder model has already been described. In the doped case, the hopping integral has the value t_R for hole motion along the rungs and the intra-chain and diagonal hopping integrals are of equal strength t. The latter assumption is crucial for the exact solvability of the eigenvalue problem in the one and two hole sectors. Though the model differs from the standard $t-J$ ladder model (the diagonal couplings are missing in the latter), the spin and charge excitation spectra exhibit similar features. In particular, the dispersion relation of the two-hole bound state branch is obtained exactly and the exact ground state is shown to be a bound state of two holes with $K=0$ and $d-$wave type symmetry. The ladder exists in the Luther-Emery phase. There is no spin charge separation. as in the case of a LL. In the exact hole eigenstates, the hole is always accompanied by a free spin$-\frac{1}{2}$. The hole-hole correlation function can also be calculated exactly. When $J_R \gg J$, the holes of a bound pair are predominantly on the same rung. For lower values of J_R, the holes prefer to be on n.n. rungs so that energy gain through the delocalization of a hole along the rung is possible.

The t-J ladder model constructed by Bose and Gayen is not integrable. Frahm and Kundu [84] have constructed a $t-J$ ladder model which is integrable. The Hamiltonian is given by

$$H = \sum_a H_{t-J}^{(a)} + H_{int} + H_{rung} - \mu \widehat{n} \tag{37}$$

The two chains of the ladder are labelled by $a=1,2$ and μ is the chemical potential coupling to the number of electrons in the system. $H_{t-J}^{(a)}$ is the $t-J$ Hamiltonian (Eq.(35)) for a chain plus the terms $n_j^{(a)}+n_{j+1}^{(a)}$where $n_j^{(a)}$is the total number of electrons on site j.

$$H_{int} = -\sum_j \left[H_{t-J}^{(1)}\right]_{jj+1} \left[H_{t-J}^{(2)}\right]_{jj+1} \tag{38}$$

H_{rung} includes the $t-J$ Hamiltonian (Eq. (35)) corresponding to a rung and a Coulomb interaction term $V\sum_j n_j^{(1)}n_j^{(2)}$. The possible basis states of a rung are the following. When no hole is present, a rung can be in a singlet or a triplet spin configuration. When a single hole is present, the rung is in a bonding ($|\sigma_+\rangle$) or antibonding ($|\sigma_-\rangle$) state with $|\sigma_\pm\rangle \equiv \frac{1}{\sqrt{2}}(|\sigma 0\rangle \pm |0\sigma\rangle)$ and $\sigma =\uparrow$ or $\downarrow$. The rung can further be occupied by two holes. Frahm and Kundu have studied the phase diagram of the ladder model at low temperatures and in the strong coupling regime $J_R \gg 1, V \gg \mu + |t_R|$ near half-filling. In this regime, the triplet states are unfavourable. By excluding the triplet states and choosing $J = 2t = 2$, the Hamiltonian H (Eq.(37)) can be rewritten as

$$H = -\sum_j \Pi_{jj+1} - \sum_{l=1}^{5} A_l N_l + const. \tag{39}$$

where $N_l, l = 1, 2(3, 4)$ is the number of bonding (antibonding) single hole rung states with spin $\uparrow, \downarrow$ and N_5 is the number of empty rungs. If L is the total number of rungs in the ladder, the remaining $N_0 = L - \sum_l N_l$ rungs are in singlet spin configurations. The permutation operator Π_{jk} interchanges the states on rungs j and k. If both the rungs are singly occupied by a hole, an additional minus sign is obtained on interchanging the rung states. The potentials A_l's are:

$$A_1 = A_2 \equiv \mu_+ = t_R - \mu + V \tag{40}$$

$$A_3 = A_4 \equiv \mu_- = -t_{R-}\mu + V \tag{41}$$

$$A_5 \equiv \widetilde{V} = -2\mu + V \tag{42}$$

The nature of the ground state and the low-lying excitation spectrum depends on the relative strengths of the potentials A_l's. The Hamiltonian (39) is BA solvable. The phase diagram V vs. the hole concentration n_h has been computed for $\mu_+ = \mu_-$,i.e., $t_R = 0$. For large repulsive V, the ground state can be described as a Fermi sea of single hole states $|\sigma_\pm\rangle$ propagating in a background of rung dimer states $|s\rangle$. The double-hole rung states $|d\rangle$ are energetically favourable for sufficiently strong attractive rung interactions. In the intermediate region, both types of hole rung states are present. In the frustrated $t-J$ ladder model studied by Bose and Gayen [83], the exact two-hole ground state is a linear combination of single-hole and double-hole rung states propagating in a background of rung dimer states. The single-hole rung states are the bonding states.

In a remarkable paper, Lin et al [85] have considered the problem of electrons hopping on a two-chain ladder. The interaction between the electrons is sufficiently weak and finite-ranged. At half filling, a perturbative renormalization group (RG) calculation shows that the model scales onto the Gross-Neveu (GN) model which is integrable and has $SO(8)$ symmetry. At half filling, the two-chain ladder is in the Mott insulating phase with d-wave pairing correlations. The insulating phase is further a QSL. The integrability has been utilised to determine the exact energies and quantum numbers of all the low energy excitations which constitute the degenerate $SO(8)$ multiplets. The lowest-lying excitations can be divided into three octets all with a non-zero gap (mass gap) m. Each excitation has a dispersion $\epsilon_1(q) = \sqrt{m^2+q^2}$ where q is the momentum variable measured w.r.t. the minimum energy value. One octet consists of two-particle excitations: two charge $\pm 2e$ Cooper pairs around zero momentum, a triplet of $S = 1$ magnons around momentum (π, π) and three neutral $S = 0$ particle-hole pair excitations. $SO(8)$ transformations rotate the components of the vector multiplet into one another unifying the excitations in the process. The $SO(5)$ subgroup which rotates only the first five components of the vector is the symmetry proposed by Zhang [86] to unify antiferromagnetism and superconductivity in the cuprates. The vector octet is related by a triality symmetry to two other octets with mass gap m. The 16 particles of these two octets have the features of quasi-electrons and quasi-holes. Above the 24 states with mass gap m, there are other higher-lying "bound" states with mass gap $\sqrt{3}m$. Finally, the continuum of scattering states occurs above the energy $2m$. Lin et al has further studied the effects of doping a small concentration of holes into the Mott insulating phase. In this limit, the effect of doping can be incorporated in the GN model by adding a term $-\mu Q$ to the Hamiltonian, μ being the chemical potential and Q the total charge. Integrability of the GN model is not lost as Q is a global $SO(8)$ generator. Doping is possible only for $2\mu > m$ when Cooper pairs enter the

system. The doped ladder exists in the Luther-Emery phase, whereas in the half-filled insulating limit both the spin and charge excitations are gapped. In the doped phase, the Cooper pairs can transport charge and quasi-long-range $d-$wave SC pairing correlations develop in the system. The other features of the standard $t-J$ ladder model, e.g., the discontinuous evolution of the SG on doping is reproduced. The lowest triplet excitation is a bound state of a $S=1$ magnon with a Cooper pair. As mentioned before, a similar result has been obtained numerically in the case of the standard $t-J$ ladder [82]. The triplet excitation belongs to the family of 28 excitations with mass gap $\sqrt{3}m$. If x denotes the dopant concentration, then the SG jumps from $\Delta_S(x=0)=m$ to $\Delta_S(x=0^+)=(\sqrt{3}-1)m$ upon doping. The integrability of the weakly-interacting two-chain ladder model has yielded a plethora of exact results which illustrate the rich physics associated with undoped and doped ladders.

4 Concluding Remarks

Integrable models have a dual utility. They serve as testing grounds for approximate methods and techniques. Also, they are often models of real systems and provide rigorous information about the physical properties of such systems. Integrable models are sometimes more general than what are required to describe real systems. In such cases, an integrable model corresponds to an exactly solvable point in the general phase diagram. The point may be a quantum critical point at which transition from one quantum phase to another occurs or the integrable model may be in the same phase as a more realistic model. In the latter case, the physical properties of the two models are similar. In this review, we have discussed the physical basis of some integrable spin models with special focus on the relevance of the models to real systems. The Heisenberg spin chain is probably the best example of the essential role played by exact solvability in correctly interpreting the experimental data. The concept of spinons owes its origin to the exact analysis of the BA equations. The theoretical prediction motivated the search for real spin systems in which experimental confirmation could be made. In this review, examples are also given of systems for which the links between integrable models and experimental results are not well established. A major portion of the review is devoted to physical systems which exhibit rich phenomena, like the systems with both spin and orbital degrees of freedom and undoped and doped spin ladder systems, where the need for integrable systems is particularly strong. These systems exhibit a variety of novel phenomena a proper understanding of which should be based on rigorous theory. Two-dimensional spin systems with QSL ground states have been specially mentioned to explain the recent interest in constructing integrable models of such systems. The review is meant to be an elementary introduction to the genesis and usefulness of integrable models vis-à-vis physical spin systems. Future challenges are also highlighted to motivate further research on integrable models.

There are some AFM spin models which are not integrable but for which the ground states and in some cases the low-lying excited states are known exactly. The most prominent amongst these are the Majumdar-Ghosh (MG) chain [81] and the AKLT [54] model respectively. The MG Hamiltonian is defined in 1d for spins of magnitude $\frac{1}{2}$. The Hamiltonian includes both n.n. as well as n.n.n. interactions. The strength of the latter is half that of the former. The exact ground state is doubly degenerate and the states consist of singlets along alternate links of the lattice. The excitation spectrum is not exactly known and has been calculated on the basis of a variational wave function [88]. Generalizations of the MG model to 2d with exactly-known ground states are possible [39, 89, 90, 91]. The Shastry-Sutherland model [89] is of much current interest due to the recent discovery of the compound $SrCu_2(BO_3)_2$ which is well-described by the model [92]. Some of these models including the AKLT model have been reviewed in the references [93, 94, 95, 96] from which more information about the models can be obtained. These models incorporate physical features of real systems and provide valuable insight on the magnetic properties of low-dimensional quantum spin systems. The models supplement integrable models in obtaining exact information and provide motivation for the construction of integrable generalisations.

References

[1] H.Bethe, Z.Physik 71, 205 (1931); see also The Many Body Problem: An Encyclopedia of Exactly Solved Models in One Dimension ed. by D. C. Mattis (World Scientific 1993) for an English translation of Bethe's paper.

[2] L. A. Takhtajan and L. D. Faddeev, Russian Mathematical Surveys 34:5, 11 (1979); L. D. Faddeev, Sov. Sci. Rev. C1, 107 (1980)

[3] E. Lieb and W. Liniger, Phys. Rev. 130, 1605 (1963); E. Lieb, Phys. Rev. 130, 1616 (1963); M. Gaudin, Phys. Lett. 24A, 55 (1967); C. N. Yang and C. P. Yang, J. Math. Phys. 10, 1115 (1969)

[4] E. Lieb and F. Y. Wu, Phys. Rev. Lett. 20, 1445 (1968)

[5] B. Sutherland, Phys. Rev. Lett. 34, 1083 (1975); ibid 35, 185 (1975)

[6] B. Sutherland, Phys. Rev. B 12, 3795 (1975)

[7] N. Andrei, Phys. Rev. Lett. 45, 379 (1980)

[8] P. B. Wiegmann, J. Phys. C 14, 1463 (1981); V. M. Filyov, A. M. Tsvelick and P. G. Wiegmann, Phys. Lett. 81A, 175 (1981)

[9] P. A. Bares and G. Blatter, Phys. Rev. Lett. 64, 2567 (1990)

[10] Quantum Electron Liquids and High$-T_c$ Superconductivity by T. González, M. A. Martin-Delgado, G. Sierra and A. H. Vozmediano (Springer-Verlag, Berlin Heidelberg 1995), Chapter 10

[11] B. Sutherland in Exactly Solvable Problems in Condensed Matter and Relativistic Field Theory ed. by B. S. Shastry, S. S. Jha and V. Singh (Springer-Verlag, Berlin Heidelberg 1985), p. 1

[12] M. Gaudin, Phys. Rev. Lett. 26, 1301 (1971)

[13] L. A. Takhtajan in Exactly Solvable Problems in Condensed Matter and Relativistic Field Theory ed. by B. S. Shastry, S. S. Jha and V. Singh (Springer-Verlag, Berlin Heidelberg 1985), p. 175

[14] N. M. Bogoliubov, A. G. Izergin and V. E. Korepin in Exactly Solvable Problems in Condensed Matter and Relativistic Field Theory ed. by B. S. Shastry, S. S. Jha and V. Singh (Springer-Verlag, Berlin Heidelberg 1985), p. 220; see also V. E. Korepin, N.M. Bogoliubov and A. G. Izergin, QISM and Correlation Functions (Cambridge University Press 1993)

[15] Yu. A. Izyumov and Yu. N. Skryabin, Statistical Mechanics of Magnetically Ordered Systems (consultants Bureau, New York 1988), Chapter 5 and references therein

[16] H. B. Thacker, Rev. Mod. Phys. 53, 253 (1981)

[17] A. Kundu, Indian J. Phys. 72B, 283 (1998)

[18] R. J. Baxter, Ann. Phys. 70, 323 (1972)

[19] J. D. Johnson, S. Krinsky and B. M. McCoy, Phys. Rev.A 8, 2526 (1973)

[20] J. B. Torrance and M. Tinkham, Phys. Rev. 187, 587 (1969); ibid 187, 59 (1969)

[21] D. F. Nicoli and M. Tinkham, Phys. Rev. B 9, 3126 (1974)

[22] M. Karbach, K. Hu and G. Müller, Comp. in Phys. 12, 565 (1998) (cond-mat/9809163)

[23] L. D. Faddeev and L. A. Takhtajan, Phys. Lett. 85A, 375 (1981); see also C. K. Majumdar in Exactly Solvable Problems in Condensed Matter and Relativistic Field Theory ed. by B. S. Shastry, S. S. Jha and V. Singh (Springer-Verlag, Berlin Heidelberg 1985), p. 142

[24] D. A. Tennant, T. G. Perring, R. A. Cowley and S. E. Nagler, Phys. Rev. Lett. 70, 4003 (1993)

[25] G. Müller, Phys. Rev. B 26, 1311 (1982); M. Mohan and G. Müller, Phys. Rev. B 27, 1776 (1983)

[26] A. H. Bougourzi, M. Karbach and G. Müller, Phys. Rev. B 57, 11429 (1998)

[27] M. Karbach et al., Phys. Rev. B 55, 12510 (1997)

[28] D. A. Tennant, R. A. Cowley, S. E. Nagler and A. M. Tsvelik, Phys. Rev. B 52, 13368 (1995); D. C. Dender et al., Phys. Rev. B 53, 2583 (1996); R. Coldea et al., Phys. Rev. Lett. 79, 151 (1997); P. R. Hammar et al., Phys. Rev. B 59, 1008 (1999)

[29] M. Arai et al., Phys. Rev. Lett. 77, 3649 (1996); K. Fabricius et al., Phys. Rev. B 57, 1102 (1998)

[30] S. E. Nagler, W. J. L. Buyers, R. L. Armstrong and B. Briat, Phys. Rev. B 27, 1784 (1983); ibid 28, 3873 (1983); W. J. Buyers, M. J. Hogan, R. L. Armstrong and B. Briat, Phys. Rev. B 33, 1727 (1986)

[31] N. Ishimura and H. Shiba, Prog. Theor. Phys. 63, 745 (1980)

[32] I. Bose and S. Chatterjee, J. Phys. C: Solid State Physics 16, 947 (1983)

[33] I. Bose and A. Ghosh, J. Phys.: Condens. Matter 8, 351 (1996); F. Matsubara and S. Inawashiro, Phys. Rev. B 43, 796 (1991); J. P. Goff, D. A. Tennant and S. E. Nagler, Phys. Rev. B 52, 15992 (1995)

[34] F. D. M. Haldane, Phys. Rev. Lett. 60, 635 (1988); B. S. Shastry, Phys. Rev. Lett. 60, 639 (1988); see also Quantum Many-Body Systems in One Dimension by Z. N. C. Ha (World Scientific 1996)

[35] P. W. Anderson,Mater. Res. Bull. 8, 153 (1973); see also P. Fazekas and P. W. Anderson, Phil. Mag. 30, 432 (1974)

[36] The Theory of Superconductivity in the High$-T_c$ Cuprates by P. W. Anderson (Princeton University Press, Princeton 1997)

[37] Exactly Solvable Models of Strongly Correlated Electrons ed. by V. E. Korepin, F. H. L. Eβler (World Scientific 1994)

[38] D. A. Huse and V. Elser, Phys. Rev. Lett. 60, 2531 (1988); B. Bernu, C. Lhuillier and L. Pierre, Phys. Rev. Lett. 69, 2590 (1992)

[39] I. Bose, Phys. Rev. B 45, 13072 (1992); I. Bose and A. Ghosh, Phys. Rev. B 56, 3149 (1997)

[40] D. S. Rokhsar and S. Kivelson, Phys. Rev. Lett. 61, 2376 (1988)

[41] R. Moessner and S. Sondhi, Phys. Rev. Lett. 86, 1881 (2001)

[42] C. Nayak and K. Shtengel, Phys. Rev. B 6406, 4422 (2001); L. Balents, M. P. A. Fisher and S. M. Girvin, cond-mat/0110005

[43] A. Kitaev, quant-ph/9707021

[44] R. Coldea et al., Phys. Rev. Lett. 86, 1335 (2001); R. Coldea et al., cond-mat/0111079

[45] T. Moriya, Magnetism ed. by G. T. Rado and H. Suhl (New York: Academic 1963)

[46] S. W. Cheong, J. D. Thompson and Z. Fisk, Phys. Rev. B 39, 4395 (1989)

[47] M. Oshikawa and I. Affleck, Phys. Rev. Lett. 79, 2883 (1997)

[48] F. C. Alcaraz and W. F. Wreszinski, J. Stat. Phys. 58, 45 (1990)

[49] L. A. Takhtajan, Phys. Lett. 87A, 479 (1982); H. M. Babujian, Phys. Lett. 90A, 479 (1982)

[50] E. Lieb, T. D. Scultz and D. C. Mattis, Ann. Phys. 16, 407 (1961)

[51] F. D. M. Haldane, Phys. Rev. Lett. 50, 1153 (1983); Phys. Lett. A 93, 464 (1983)

[52] G. E. Granroth et al., Phys. Rev. Lett. 77, 1616 (1996)

[53] F. Mila and F. C. Zhang, cond-mat/0006068

[54] I. Affleck, T. Kennedy, E. H. Lieb and H. Tasaki, Phys. Rev. Lett. 59, 799 (1987)

[55] J. F. Di Tusa et al., Phys. Rev. Lett. 73, 1857 (1994)

[56] G. Xu et al., Science 289, 419 (2000); see also I. Bose and E. Chattopadhyay, Int. J. Mod. Phys. B 15, 2535 (2001)

[57] H. Frahm, M. P. Pfannmüller and A. M. Tsvelik, Phys. Rev. Lett. 81, 2116 (1998)

[58] H. Frahm and C. Sobiella, Phys. Rev. Lett. 83, 5579 (1999)

[59] Y. Tokura and N. Nagaosa, Science 288, 462 (2000); D. I. Khomskii and G. A. Sawatzky, Solid State Comm. 102, 87 (1997)

[60] D. I. Khomskii, Int. J. Mod. Phys. B 15, 2665 (2001)

[61] A. K. Kolezhuk and H. J. Mikeska, Phys. Rev. Lett. 80, 2709 (1998)

[62] E. Axtell, T. Ozawa, S. Kauzlarich and R. R. P. Singh, J. Solid State Chem. 134, 423 (1997); M. Isobe and Y. Ueda, J. Phys. Soc. Jpn. 65, 1178 (2996); Y. Fujii et al., ibid 66, 326 (1997)

[63] P. B. Allen and V. Perebeinos, Nature 410, 155 (2001)

[64] E. Saitoh et al., Nature 410, 180 (2001)

[65] E. Dagotto, Rep. Prog. Phys. 62, 1525 (1999)

[66] E. Dagotto and T. M. Rice, Science 271, 618 (1996)

[67] M. Windt et al., cond-mat/0103438

[68] T. M. Rice, S. Gopalan and M. Sigrist, Europhys. Lett. 23, 445 (1993)

[69] M. Azuma et al., Phys. Rev. Lett. 73, 3463 (1994)

[70] B. C. Watson et al., cond-mat/0011052

[71] I. Bose and S. Gayen, Phys. Rev. B 48, 10653 (1993)

[72] Y. Xian, Phys. Rev. B 52, 12485 (1995)

[73] A. K. Kolezhuk and H. J. Mikeska, Int. J. Mod. Phys. B 12, 2325 (1998)

[74] H. Frahm and C. Rödenbeck, Europhys. Lett. 33, 47 (1996); H. Frahm and C. Rödenbeck, J. Phys. A: Math. Gen. 30, 4467 (1997); S. Albeverio, S. M. Fei and Y. Wang, Europhys. Lett. 47, 364 (1999); M. T. Batchelor and M. Maslen, J. Phys. A: Math. Gen. 32, L377 (1999); A. P. Tonel et al., cond-mat/0105302 and references therein

[75] Y. Wang, Phys. Rev. B 60, 9236 (1999)

[76] J. Ornstein and A. J. Millis, Science 288, 468 (2000)

[77] E. Dagotto, J. Riera and D. Scalapino, Phys. Rev. B 45, 5744 (1992)

[78] M. Uehara et al., J. Phys. Soc. Jpn. 65, 2764 (1996)

[79] H. Tsunetsugu, M. Troyer and T. M. Rice, Phys. Rev. B 49, 16078 (1994)

[80] M. Troyer, H. Tsunetsugu and T. M. Rice, Phys. Rev. B 53, 251 (1996)

[81] C. Jurecka and W. Brenig, cond-mat/0107365

[82] D. Poilblanc et al., Phys. Rev. B 62, R14633 (2000)

[83] I. Bose and S. Gayen, J. Phys.: Condens. Matter 6, L405 (1994); ibid 11, 6427 (1999)

[84] H. Frahm and A. Kundu, J. Phys. : Condens. Matter 11, L557 (1999)

[85] H. Lin, L. Balents and M. P. A. Fisher, Phys. Rev. B 58, 1794 (1998)

[86] S. C. Zhang, Science 275, 1089 (1997)

[87] C. K. Majumdar and D. K. Ghosh, J. Math. Phys. 10, 1388, 1399 (1969) ; C. K. Majumdar, J. Phys. C 3 , 911 (1970)

[88] B. S. Shastry and B. Sutherland, Phys. Rev. Lett. 47, 964 (1981)

[89] B. S. Shastry and B. Sutherland, Physica B 108, 1069 (1981)

[90] I. Bose and P. Mitra, Phys. Rev. B 44, 443 (1991); see also U. Bhaumik and I. Bose, Phys. Rev. B 52, 12489 (1995); A. Ghosh and I. Bose, Phys. Rev. B 55, 3613 (1997)

[91] R. Siddharthan, Phys. Rev. B 60, R9904 (1999); B. Kumar, cond-mat/0205072

[92] S. Miyahara and K. Ueda, Phys. Rev. Lett. 82, 3701 (1999)

[93] I. Bose in Field Theories in Condensed Matter Physics ed. by S. Rao (Hindustan Book agency, India 2001), p. 359

[94] Interacting Electrons and Quantum Magnetism by A. Auerbach (Springer-Verlag, New York 1994)

[95] I. Affleck, J. Phys.: Condens. Matter 1, 3047 (1989)

[96] Quantum magnets: a brief overview, by I. Bose, cond-mat/0107399